catalysts

MDPI

Article

Comparative Studies of Fischer-Tropsch Synthesis on Iron Catalysts Supported on Al_2O_3-Cr_2O_3 (2:1), Multi-Walled Carbon Nanotubes or BEA Zeolite Systems

Pawel Mierczynski [1,*], Bartosz Dawid [1], Karolina Chalupka [1], Waldemar Maniukiewicz [1], Izabela Witoska [1], Krasimir Vasilev [2] and Malgorzta I. Szynkowska [1]

[1] Institute of General and Ecological Chemistry, Lodz University of Technology, Zeromskiego 116, Lodz 90–924, Poland
[2] School of Engineering, University of South Australia, Mawson Lakes 5095, Australia
* Correspondence: pawel.mierczynski@p.lodz.pl; Tel.: +48-42-631-31-25

Received: 30 May 2019; Accepted: 8 July 2019; Published: 15 July 2019

Abstract: The main goal of the presented paper is to study the influence of a range of support materials, i.e., multi-walled carbon nanotubes (MWCNTs), Al_2O_3-Cr_2O_3 (2:1), zeolite β-H and zeolite β-Na on the physicochemical and catalytic properties in Fischer-Tropsch (F-T) synthesis. All tested Fe catalysts were synthesized using the impregnation method. Their physicochemical properties were extensively investigated using various characterization techniques such as the Temperature-Programmed Reduction of hydrogen (TPR-H_2), X-ray diffraction, Temperature-Programmed Desorption of ammonia (TPD-NH_3), Temperature-Programmed Desorption of carbon dioxide (TPD-CO_2), Fourier transform infrared spectrometry (FTIR), Brunauer Emmett Teller method (BET) and Thermogravimetric Differential Analysis coupled with Mass Spectrometer (TG-DTA-MS). Activity tests were performed in F-T synthesis using a high-pressure fixed bed reactor and a gas mixture of H_2 and CO (50% CO and 50% H_2). The correlation between the physicochemical properties and reactivity in F-T synthesis was determined. The highest activity was from a 40%Fe/Al_2O_3-Cr_2O_3 (2:1) system which exhibited 89.9% of CO conversion and 66.6% selectivity toward liquid products. This catalyst also exhibited the lowest acidity, but the highest quantity of iron carbides on its surface. In addition, in the case of iron catalysts supported on MWCNTs or a binary oxide system, the smallest amount of carbon deposit formed on the surface of the catalyst during the F-T process was confirmed.

Keywords: hydrogenation of CO; iron catalysts; syngas; monometallic iron catalysts

1. Introduction

Fischer-Tropsch synthesis is a promising catalytic route for the environmentally friendly production of fuels from biomass, coal and natural gas [1–5]. However, on an industrial scale, a very efficient and stable catalyst is desirable. The catalyst activity and selectivity are influenced by the nature and structure of the carrier material, metal dispersion, the nature of metal, metal loading, and to a large extent, it depends on the methodology of preparation [6]. Metallic catalysts in Fischer-Tropsch synthesis are often supported on oxides, zeolites or binary oxides systems and, more recently, on carbon-based systems such as activated carbon and carbon nanotubes (CNT) [7–9]. In particular, there is a growing interest in carbon nanotubes and their application as a F-T catalyst support [10,11]. Carbon nanotubes are exciting due to their unique original chemical, physical, optical and electron properties. Their special structure offers a high surface area and the presence of various defects which offer the possibility to introduce functional groups. The introduced functional groups can generate

specific physicochemical properties of the material and improve the interaction between the metal particles incorporated into their surfaces, thereby forming new catalytic systems. Zhang et al. [12] studied iron catalysts supported on the MWCNTs system in the Fischer-Tropsch process and they reported a high selectivity towards C_2–C_7 hydrocarbons but low CO conversions values. In addition, the usage of carbon nanofibers as a catalyst support in the F-T process was also investigated [13] and reported to have high stability. It is well known that acidic zeolite or other acidic supports present good performance in the F-T reaction and high selectivity to isoparaffin and unsaturated compounds generated in the final product [4,14,15]. In our previous works, iron catalysts supported on BEA zeolites and binary oxide (Al_2O_3-Cr_2O_3 (2:1)) were investigated in Fischer-Tropsch synthesis. It was proven that the dealumination process of zeolite BEA and the increase of the content of iron in the catalytic material improves the catalyst activity in the case of the process carried out on the Fe catalyst supported on the zeolite BEA [4]. In addition, the influence of the binary oxide carrier composition of iron catalysts on their reactivity properties was studied and the results also showed that the increase of Fe loading and the content of Al_2O_3 in the catalytic system lead to an increase of CO conversion in the hydrogenation process [2]. The obtained results in the F-T process also showed that the activation condition has a large impact on the catalytic properties of iron catalysts in the F-T reaction. It was proven that the Fe catalyst which was previously activated in a mixture of 50% CO and 50% H_2 exhibited the highest activity and selectivity towards liquid product formation and this effect was explained by the highest quantity of iron carbide phases present on the catalyst surface after the activation process [16]. The novelty of this work is related to the comparison studies of high active iron catalysts supported on various supports such as MWCNTs, zeolite BEA and binary oxide in Fischer-Tropsch synthesis. Additionally, the correlation between their reactivity and physicochemical properties in the investigated process was found. In addition, in the presented paper, a highly active and stable Fe/MWCNTs catalytic system was prepared and tested in the hydrogenation process of CO.

The product of the Fischer-Tropsch (F-T) process mostly contains linear paraffin, whose distribution is varied from CH_4 to long-chain hydrocarbons and obeys the Anderson–Schulz–Flory (ASF) law [17]. It is particularly desirable to obtain a final hydrocarbon product having 5 to 11 carbon atoms in a molecule containing mostly isoparaffin and olefin as gasoline range liquid fuels with a high-octane value are an important fuel in the petrochemical industry. In addition, the liquid fraction containing hydrocarbons with 10 to 21 carbon atoms in a molecule is also attractive because they are the main components in diesel. That is why the main idea of the Fischer-Tropsch reaction is to generate fuel fraction (gasoline or diesel) on a highly active, stable and selective heterogeneous catalyst, which is beneficial from the point of view of generating clean fuel. In order to achieve a liquid product containing gasoline or diesel fractions, it is strongly recommended to use them in the process of bi-functional catalysts which should have acid and metallic centres on the surface. A high yield of the fuel fraction production along with a satisfactory selectivity of the desired products is also required [18–20]. Both of these features can be achieved using bifunctional catalysts. One of the main reasons for the deactivation of Fischer-Tropsch catalysts is the deposition of carbon [5,21,22]. The formations on the catalyst surface carbon deposit blocks the active sites of the catalyst, leading to its deactivation [23]. Menon reported that the Fischer-Tropsch synthesis is a carbon insensitive reaction due to the fact that there is sufficient hydrogen on the catalyst surface for the hydrogenation of the carbon present on the catalyst surface in order to keep the surface a free surface of the catalyst [24]. Therefore, in order to regenerate the deactivated catalyst, it should be previously oxidized and then reduced to remove the carbidic and surface carbon [25].

Based on the above-presented suggestions, the main aim of the work was to carry out comparative investigations of iron systems for the Fischer-Tropsch process and reveal the link between their physicochemical and catalytic properties. It is well known that the catalytic activity of heterogeneous catalysts in the chemical process depends on the nature, dispersion and reactivity of the active centres in relation to the substrates; on the steric effects and diffusion of the reagents; and on the created products in the catalytic material pores [5]. That is why, in our studies, we used various support

materials whose structure can affect the transport of reagents and products from and to the catalyst bed with different specific surface areas and various reducing and acidic properties. In order to avoid steric effects, the carrier material should have a unified pore system which plays a crucial role during the process and directly influences the catalyst selectivity in the F-T process.

2. Results and Discussion

2.1. Influence of the Catalytic Material Composition on the Catalytic Reactivity of Monometallic Iron Catalysts in the Hydrogenation of CO

The catalytic measurements performed in the hydrogenation process showed that the distribution of the hydrocarbons in the final product depends strongly on the support used for the catalytic system. The catalytic activity results expressed as CO conversion and product selectivity in Fischer-Tropsch synthesis are given in Table 1. The obtained catalytic activity results confirmed that the most active catalyst was the 40%Fe/Al_2O_3-Cr_2O_3 (2:1) system which exhibited approximately 90% of CO conversion and high selectivity towards the liquid product (66.6%). In addition, the smallest amount of CO_2 was created in the final product obtained during the F-T reaction using this catalyst, which means that the WGS process runs in a limited way. Furthermore, in the case of the 40%Fe/Zeolite β-H and 40%Fe/MWCNT catalysts, we observed CO conversion values above 71% and selectivities towards liquid product above 67%. The only difference which was observed in the final product was the amount of carbon dioxide and methane formed during the process.

Table 1. The results of the activity measurements expressed as CO conversion and selectivity towards all products of the Fischer-Tropsch (F-T) process performed at 280 °C under elevated pressure (3 MPa) from a mixture of H_2 and CO (molar ratio 1:1).

Catalysts	Conv. (%)	S_{CO2}	S_{CH4} in HCs	S_{C2-C4} in HCs	S_{C5-C9} in HCs	$S_{C10-C21}$ in HCs	Liquid	Paraffin/ Olefins	Linear/ Branched
40%Fe/MWCNT	71.1	7.6	14.3	5.9	13.0	66.8	67.5	-	4.3
40%Fe/Zeolite β-H	75.7	4.5	18.4	5.6	44.5	31.5	69.6	-	18.2
40%Fe/Zeolite β-Na	65.2	11.0	32.6	9.1	26.0	32.3	52.2	-	2.0
40%Fe/Al_2O_3-Cr_2O_3 (2:1)	89.9	2.4	16.3	5.4	17.4	60.9	66.6	17.2	4.3

In the case of the iron catalyst supported on MWCNTs, about 7.6% of the CO_2 and about 14.3% of the CH_4 were observed in the final product. In the case of the iron catalyst supported on Zeolite β-Na, the lowest value of CO conversion and the selectivity towards liquid product was observed at 65.2% and 52.2%, respectively. It is also worth noticing that in the case of this system, the highest selectivity to CH_4 (32.6%) and towards CO_2 (11%) was detected. The latter suggests that the reaction of methanation and the conversion of carbon monoxide with water vapour ran more efficiently. In addition, the stability tests for the iron catalysts were also carried out in the hydrogenation of the CO process. Figure 1 presents the carbon monoxide conversion values as a function of the reaction time for 40%Fe/Al_2O_3-Cr_2O_3 (2:1), 40%Fe/MWCNT and the iron catalysts supported on both types of zeolite BEA. The results clearly showed that all the tested catalysts exhibited stable values during 96 h of the reaction. Only in the case of the 40%Fe/Al_2O_3-Cr_2O_3 (2:1) and 40%Fe/Zeolite β-H catalysts, was a slight decrease in CO conversion values observed during the first 48 h of the process [16].

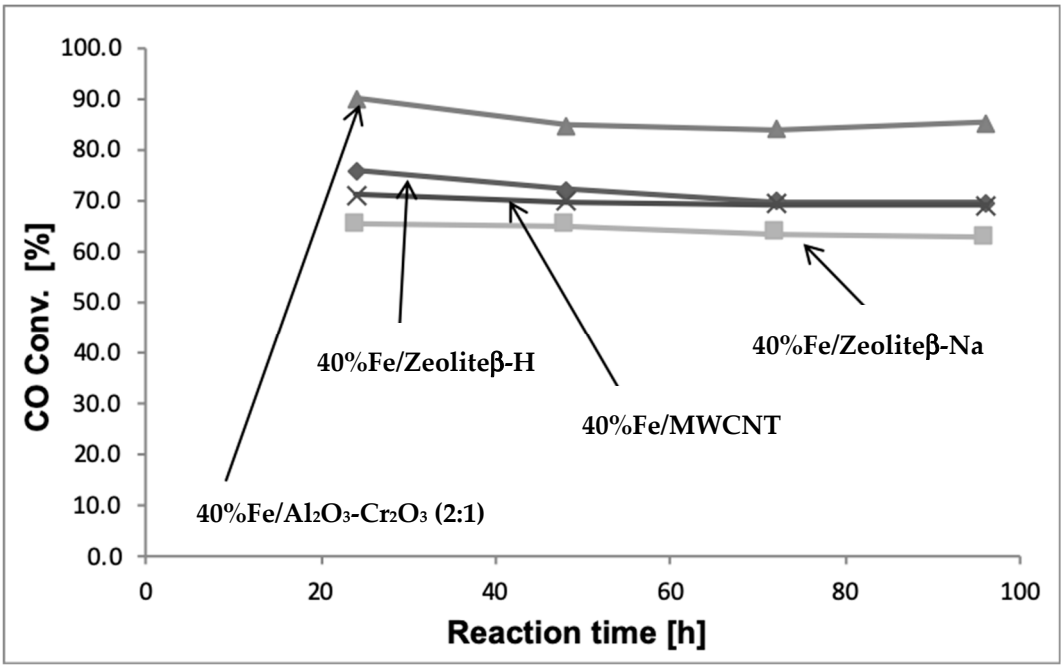

Figure 1. The carbon monoxide conversion values of iron catalysts supported on various supports obtained in the Fischer-Tropsch (F-T) process performed in a reaction mixture at 280 °C (50% H2:50% CO) at 30 atmospheres using a 2 g sample in each test.

Liquid products formed during the hydrogenation of the CO process were also analysed using GC-MS and FTIR techniques (see Figure 2). The obtained results showed that the saturated, unsaturated and branched hydrocarbons arise within the investigated process on the 40%Fe/Al_2O_3-Cr_2O_3 (2:1) catalyst. Table 1 presents the selectivity of the hydrocarbons created during the Fischer-Tropsch reaction. It is worth emphasizing that in the case of the 40%Fe/Al_2O_3-Cr_2O_3 (2:1) catalyst, the formation of unsaturated hydrocarbons was detected which were not observed when the process was carried out on the remaining catalysts. In addition, the highest quantity of the linear hydrocarbons formed in the liquid product was observed for the 40%Fe/Zeolite β-H catalyst as evidenced by the highest ratio between the linear and branched hydrocarbons (18.2). The GC-MS analysis of the liquid product obtained during the hydrogenation of CO on the 40%Fe/Zeolite β-H catalyst material gave evidence that it had a high selectivity to linear hydrocarbons. Whereas, the chromatographic analysis performed for the 40%Fe/MWCNT and 40%Fe/Al_2O_3-Cr_2O_3 (2:1) catalysts showed the ratio between linear and branched hydrocarbons to be equal to 4.3. In the case of the 40%Fe/Zeolite β-Na catalyst, the formation of lower quantities of linear hydrocarbons was observed. Figure 2 shows the FTIR analysis of the products of the hydrogenation of the CO process performed on the iron catalysts supported on various types of supports. FTIR measurements recorded for the studied Fe catalysts confirmed the presence on their surface of the following functional groups assigned to –OH stretching, –C–H stretching in alkanes, –CH_2, –CH, –CH_3 and $(CH_2)n > 4$. The presence of the bands attributed to the previously mentioned functional groups confirmed the occurrence of linear and branched hydrocarbons in the final liquid product and the GC-MS results obtained for these catalysts. In addition, the occurrence of the specific bands located on the FTIR spectrum of 40%Fe/Al_2O_3-Cr_2O_3 (2:1) assigned to C=C in alkenes, C–H in alkenes, and R–CH=CH–R were confirmed. The presence of the above listed functional groups on the spectra confirmed the chromatographic analysis and the formation of unsaturated compounds formed via the F-T process [2].

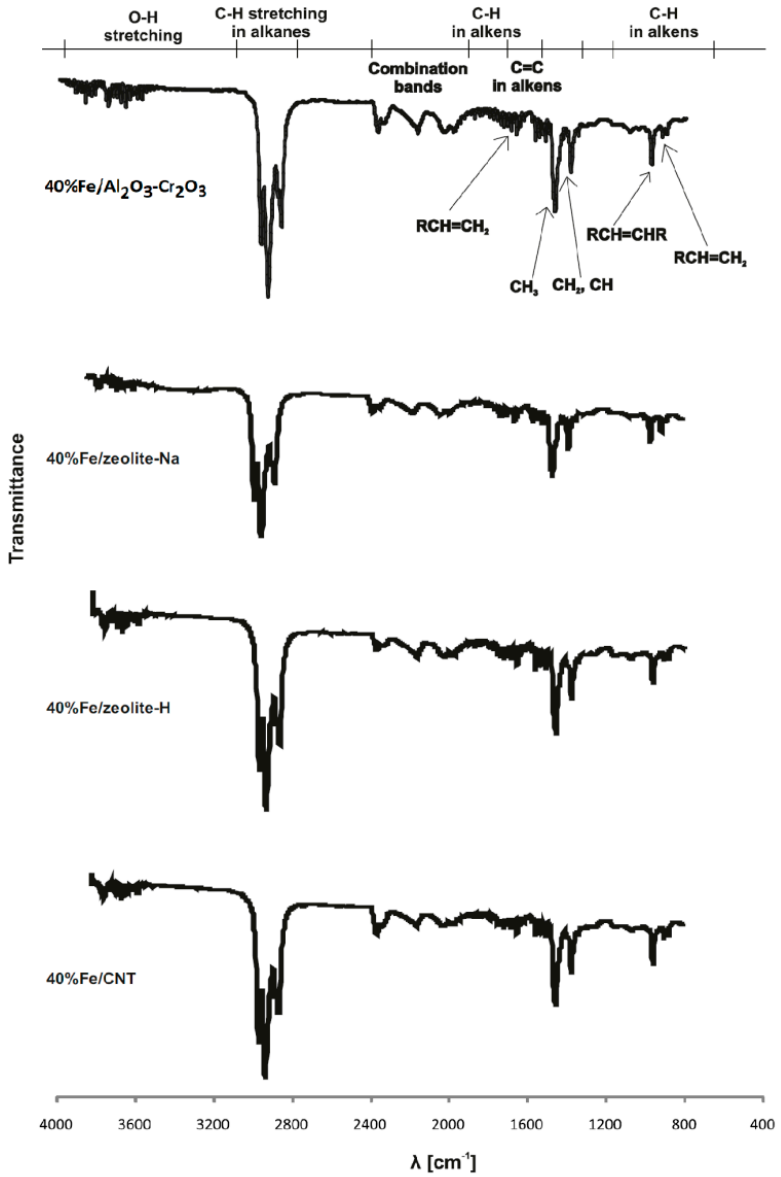

Figure 2. Fourier transform infrared spectrometry (FTIR) spectra's of the product formed in the hydrogenation of the CO process at 280 °C under elevated pressure (3 MPa) from a mixture of H_2 and CO (50% CO and 50% H_2) using Fe catalysts supported on various carriers (binary oxides, zeolite-Na, zeolite β-H and MWCNTs) calcined in an air atmosphere at 500 °C for 4 h and activated in a reaction mixture.

Table 1 also shows the distributions of the hydrocarbon fractions produced within the F-T process into gasoline and diesel expressed as $S_{C5–C9}$ and $S_{C10–C21}$. The results presented in Table 1 clearly show that in the case of the 40%Fe/MWCNT and 40%Fe/Al_2O_3-Cr_2O_3 catalysts, a diesel fraction is formed mainly. The higher quantity of the C_5–C_9 fraction in the final product was formed for the 40%Fe/Zeolite β-H and 40%Fe/Zeolite β-Na catalysts equal to 44.5% and 26.0%, respectively. It is also worth mentioning that the F-T process carried out on the 40%Fe/Zeolite β-H catalyst leads mainly to the production of a C_5–C_9 hydrocarbons fraction which means that it can be used for petrol generation. On the other hand, the reaction which was performed on iron catalysts supported on the Na form of the zeolite BEA leads mainly to the production of the same quantity of hydrocarbons, which are components of gasoline and diesel.

One of the main problems in the hydrogenation of CO is the carbon deposit formed during the process which blocks access to the active centres of the reaction. In order to study the carbon

deposit formed in the F-T process, the thermal analysis of the iron catalysts (40%Fe/Zeolite β-H, 40%Fe/Zeolite β-H, 40%Fe/MWCNT and 40%Fe/Al_2O_3-Cr_2O_3) after calcination and F-T reaction was done. The obtained TG-DTA-MS measurements are given in Figure 3 and Figure S1–S3, respectively. Figure 3 shows the mass spectrum of the gaseous products formed during the decomposition of all investigated catalysts. The amount and the form of the carbon deposit on the iron catalyst surface (40%Fe/Zeolite β-H and 40%Fe/Zeolite β-Na) are presented in Figure S1 and in Table 2. As it is seen in Figure S1, the carbon deposition is higher for the protonic form of zeolite (36.50%) than for the sodium form of zeolite (31.20%). The oxidation process of carbon occurs in two steps for both iron zeolite catalysts. Both forms of carbon deposits are easily oxidised. The oxidation proceeds up to 600 °C (Figure S1). Two visible peaks of CO_2 (MS profile, Figure 3) with a maximum at 370 °C are attributed to the removal of the surface carbides forms (FeC_2 and FeC_3) and/or filamentous carbon. This type of carbon is probably α carbon, whereas the peak with a maximum at 510 °C may be attributed to the removal of the oligomerized carbon species, which is signed as β carbon (C_β) or bulks carbides, in line with earlier reports [26,27]. In the case of the iron catalysts supported on the carbon nanotubes material (MWCNTs), we carried out TG-DTA-MS measurements for calcined and used catalysts in order to calculate the quantity of the carbon deposited on the catalyst surface (Figure S2). The TG-DTA measurements showed that iron catalyst Fe/MWCNT used in F-T had a total carbon of 67.22% while for the calcined catalyst, the total carbon which was oxidized to CO_2 was 47.11%. These results confirm that the smallest amount of carbon deposit formed after the F-T reaction (20.11) was in the case of the Fe/MWCNT system. These TG-DTA-MS results indicate that this catalytic material should exhibit the highest stability in the investigated process of the hydrogenation of CO. For iron supported on binary oxides catalysts (Figure S3), two peaks of CO_2 formation are also observed and this type of carbon is easily oxidised too. Moreover, the amount of carbon deposition is much lower than those of previously investigated catalysts and is equal to 23.45% (Table 2 and Figure S3). In all studied cases, the type of carbon deposition with a maximum at 310 °C is assigned to the removal of surface carbides forms and/or filamentous carbon (C_α), while the second peak with a maximum located at 520 °C can be assigned to the oxidation of iron carbides (C_β) [26]. It is worth noting that the main type of carbon deposition is β carbon.

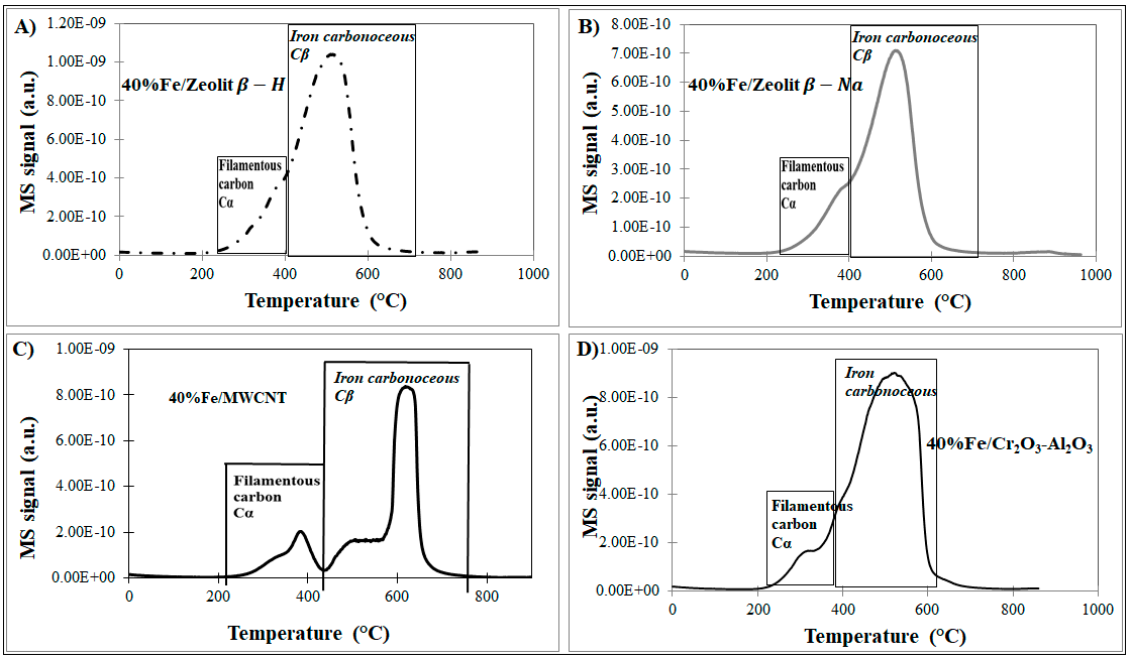

Figure 3. The mass spectrum of the gaseous decomposition products in (**A**) Fe/Zeolite β–H; (**B**) Fe/Zeolite β–Na; (**C**) Fe/MWCNT; (**D**) Fe/Al_2O_3-Cr_2O_3.

Table 2. The amount of carbon deposition on iron catalysts.

Catalyst	Amount of Carbon Deposition (%)
40%Fe/H-zeolite	36.50
40%Fe/Na-zeolite	31.20
40%Fe/MWCNT	47.11
40%Fe/MWCNT (after reaction)	67.22 (20.11 *) see Figure S2
40%Fe/Cr_2O_3-Al_2O_3	23.45

* the value in the bracket is a difference between the total carbon in the case of the 40%Fe/MWCNTs catalyst after the reaction and in the case of calcined catalyst. All measurements were done for the catalysts after 20 h of conducting the process.

2.2. Specific Surface Area (SSA) and Pore Size of the Investigated Catalytic Systems

The specific surface area (SSA) and pore sizes of the prepared systems were investigated by the BET method. The SSA measurements of Cr_2O_3-Al_2O_3 and iron catalysts are given in Table 3. The results of the SSA results showed that 40%Fe/Al_2O_3-Cr_2O_3 (2:1) catalyst exhibited the lowest values of specific surface area and pore sizes equal to 118 $m^2 \cdot g^{-1}$ and 2.6 nm, respectively. The SSA measurements obtained for the rest of the catalytic systems showed that the highest specific surface area exhibited 40%Fe/Zeolite β-Na catalyst. Iron catalysts supported on Zeolite β-H had an SSA of 256 $m^2 \cdot g^{-1}$. The pore sizes of the iron catalysts supported on the zeolite systems were practically the same, while, in the case of the 40%Fe/MWCNT system, the SSA measurements showed that the specific surface area of this system was 217 $m^2 \cdot g^{-1}$ and the pore size of this material was equal to 9.3 nm.

Table 3. The results of the specific surface area and average pore radius of iron catalysts.

Catalyst	Specific Surface Area ($m^2 \cdot g^{-1}$)	Average Pore Radius (nm)
40%Fe/MWCNT	217	9.3
40%Fe/Zeolite β-H	256	4.5
40%Fe/Zeolite β-Na	278	4.2
40%Fe/Al2O3-Cr2O3 (2:1)	118	2.6

2.3. Reduction Behaviour of Catalytic Material

The interaction between the components of the catalytic system used in Fischer-Tropsch synthesis was determined using the TPR-H_2 technique. The reduction profiles recorded for supports (MWCNTs, Al_2O_3-Cr_2O_3 (2:1)) and iron catalysts are shown in Figure 4. The TPR-H_2 profile of the MWCNTs did not show any reduction stages. In the case of the binary oxide system, only one reduction peak located in the temperature range 300–580 °C was observed, which was assigned to the reduction of Cr(VI) species formed from the previously oxidized phase of α–Cr_2O_3 [28–32].

The TPR-H_2 curves recorded for the 40%Fe/MWCNT system showed four reduction steps with the maxima of the peaks at 250, 300, 500 and 640 °C, respectively. The first reduction peak located on the TPR profile (240–260 °C) is assigned to the reduction of the surface species of Fe_2O_3 to Fe_3O_4. The second effect with the maximum situated at about 300 °C is connected with the partial reduction of Fe_3O_4 (Fe(II, III)) to the wustite phase (FeO–Fe(II)) [33–35] together with the reduction of Fe_2O_3 strongly interacting with MWCNTs. The third TPR-H_2 effect situated at a higher temperature of about 500 °C is connected with the reduction of the magnetite and wustite phases to metallic iron. The last reduction stage visible on the TPR curve above 550 °C is related to the methanation process of the MWCNTs. The TPR-H_2 profile of 40%Fe/Al_2O_3-Cr_2O_3 (2:1) presents three reduction steps with maxima at about 250, 350 and 550 °C. The first reduction stage is connected with the reduction of Fe_2O_3 to Fe_3O_4. The second reduction stage is attributed to the reduction of the Cr(VI) species and Fe_3O_4 to wustite [2]. The last reduction step presents the reduction of the wustite phase to metallic iron. The TPR-H_2 profiles of zeolite-based catalysts present two reduction stages independently on the support

form. The observed reduction stages are connected with the reduction of Fe_2O_3 to Fe_3O_4. The second peak was attributed to the reduction of magnetite to Fe^0 [33–35].

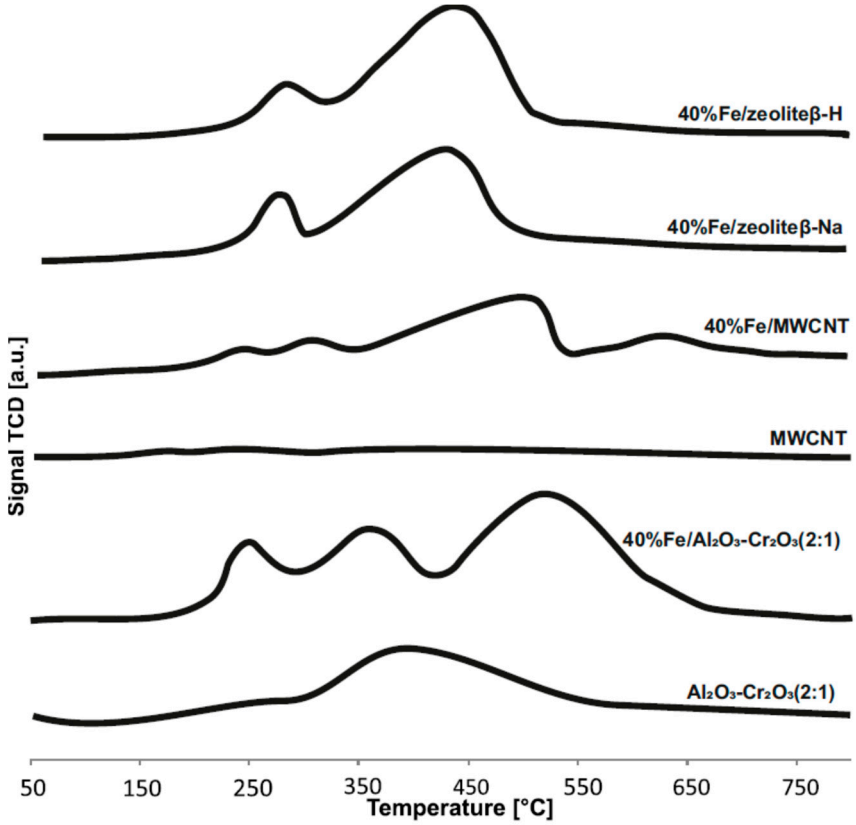

Figure 4. The temperature programmed reduction of hydrogen (TPR-H_2) curves of supports and iron catalysts supported on two types of zeolite β, MWCNTs and Al_2O_3-Cr_2O_3 (2:1).

To better understand the reducibility of the Fe/MWCNT catalyst, XRD measurements in the temperature range of 50–50 °C using a mixture of 5% H_2-95% Ar were performed. The results of the phase composition studies are given in Figure 5. The results clearly showed that starting from 50 °C, only the hematite phase on the diffraction curve recorded for this system was observed. Raising the temperature to 300 °C results in the appearance of reflexes on the XRD curve assigned to the magnetite and wustite phases. This result confirms the first reduction step of the catalytic material. A further increase of the temperature from 300 to 450 °C leads to the increase of the intensity of the diffraction peaks of wustite and the decrease of the intensity of the reflexes of magnetite. This means that at this temperature, the reduction of α-Fe_2O_3 strongly interacts with MWCNTs. Above 550 °C, on the XRD curves recorded for the investigated catalyst, only diffraction peaks assigned to the metallic iron phase was visible. This confirms the total reduction of iron oxides to Fe^0. In addition, this result also confirms the mechanism of the reduction of this system which was postulated based on the TPR reduction measurements that the last reduction stage was connected with the methanation process [36,37] of the MWCNTs. This reduction stage observed on the catalyst surface is confirmed by the lack of other crystallographic phases on the XRD curves recorded above 550 °C.

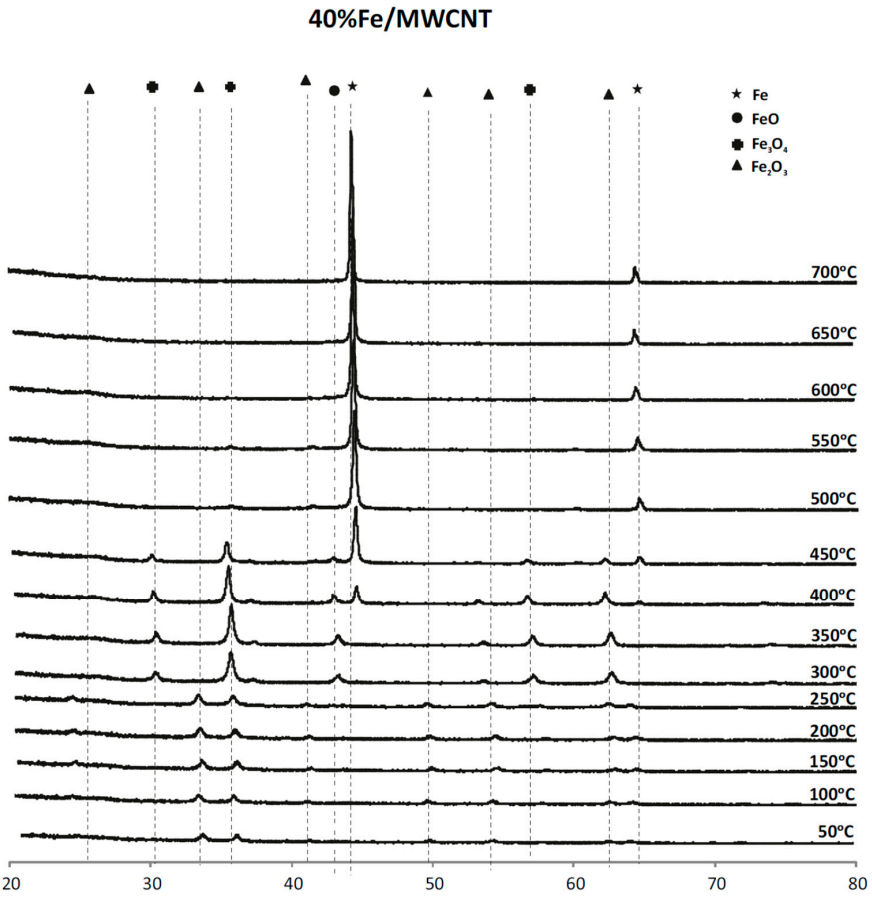

Figure 5. The X-ray diffraction patterns of the Fe/multi-walled carbon nanotube (MWCNT) catalyst collected during the reduction process carried out at a temperature range of 50–700 °C using a reducing mixture of 5% H_2-95% Ar.

2.4. Phase Composition Research of Iron Supported Catalysts

The analysis of the X-ray diffraction studies of the iron catalysts after calcination and after the reaction were studied and the results are presented in Figures 6 and 7. The X-ray analysis of the calcined samples is presented in Figure 6. The diffraction curves recorded for the calcined 40% Fe/MWCNT, 40%Fe/Zeolite β-Na and 40%Fe/Zeolite β-H catalysts confirmed the presence of the hematite and magnetite phases. Moreover, the XRD diffraction curve of the calcined 40% Fe/Al2O3-Cr2O3 (2:1) catalyst showed diffraction peaks assigned to magnetite, $FeCr_2O_4$, $FeAl_2O_4$ phases, respectively. The X-ray diffractograms recorded for the spent Fe catalysts supported on MWCNTs, Al_2O_3-Cr_2O_3 (2:1), zeolite β-H -Na and zeolite β-H are given in Figure 7. The obtained XRD results showed the occurrence of the η-Fe_2C, o-Fe_3C, h-Fe_3C, χ-Fe_5C_2 and magnetite phases on the diffraction patterns recorded for iron catalysts. XRD analysis performed for the spent catalysts did not confirm the presence of the hematite phase on the surface of the catalysts. In addition, depending on the catalyst composition, the $FeCr_2O_3$ and $FeAl_2O_4$ phases were also detected on the diffraction curves recorded for the investigated spent catalysts. It is also worth noting that the previously mentioned phases of carbides were not observed on the XRD curves recorded for the calcined catalysts. These results confirm that iron carbides are the active species of the F-T process and are created during the activation process performed in a mixture of CO and H_2 (50%CO and 50% H_2). Furthermore, the quantity of the carbides determines the catalytic activity in the investigated process. The activity tests performed in the F-T process clearly indicate that iron carbides such as η-Fe_2C, h-Fe_3C, χ-Fe_5C_2 which were created on the surface of the catalyst, are the active species in the hydrogenation of the CO reaction [38,39].

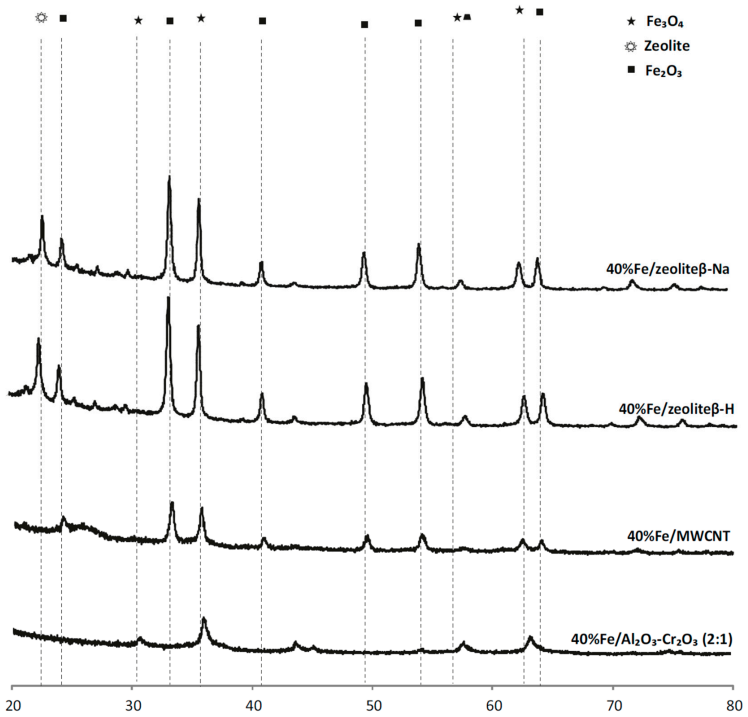

Figure 6. The X-ray diffraction patterns recorded for calcined iron catalysts supported on MWCNTs and binary oxide support.

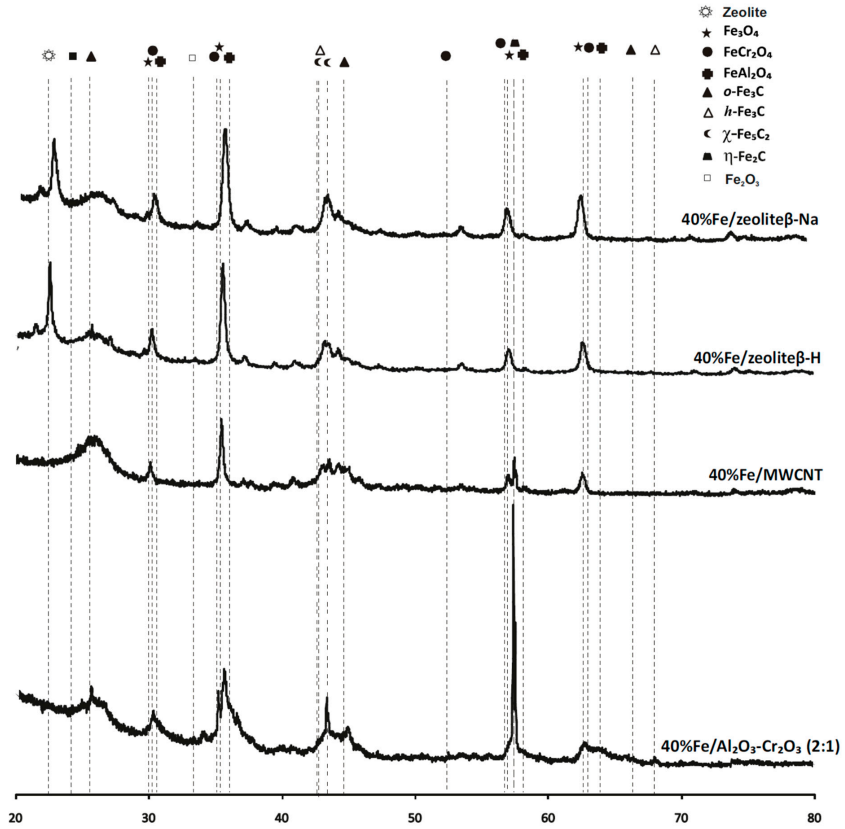

Figure 7. The X-ray diffraction patterns recorded for the spent iron catalysts supported on binary oxide, MWCNTs, zeolite β-H -Na and zeolite β-H.

2.5. The Influence of the Catalytic Support on the Acidity Properties of the Fe Based Catalysts

The acidity and the distribution of acidic centres of the investigated catalysts were determined by the TPD-NH_3 method. The distribution of acid centres on the surface of the reduced catalyst has been estimated based on the area under the desorption peaks in the temperature range 100–600 °C and the results are presented in Table 4 and Figure 8. The results of acidity measurements confirmed the existence of three types of acid centres present on the surface of the tested catalysts. The TPD-NH_3 results obtained for the investigated catalysts show that 40%Fe/MWCNT had the highest acidity and 40%Fe/Zeolite β-H had the lowest total acidity. In addition, the catalyst based on MWCNTs was characterized by a small number of weak centres and the highest quantity of medium and strong centres compared to the rest of the studied catalytic systems. Furthermore, the catalysts which were characterized by the lowest total acidity of the surface showed the highest CO conversion and high selectivity towards liquid products [4,40].

Table 4. The amount of NH_3 adsorbed on the surface of the reduced 40%Fe/MWCNT (multi-walled carbon nanotube), 40%Fe/Zeolite β-H, 40%Fe/Zeolite β-Na and 40%Fe/Al_2O_3-Cr_2O_3 (2:1) catalysts (reduction for 1 h in a mixture of 5%H_2-95%Ar at 500 °C) calculated from the temperature programmed desorption (TPD-NH_3) measurements.

Catalysts/Supports	Weak Centres (mmol g^{-1})	Medium Centres (mmol·g^{-1})	Strong Centres (mmol·g^{-1})	The Total Amount of Desorbed NH_3 (mmol·g^{-1})
40%Fe/Al_2O_3-Cr_2O_3 (2:1)	0.07	0.09	0.09	0.25
40%Fe/Zeolite β-H	0.22	0.11	0.07	0.40
40%Fe/Zeolite β-Na	0.34	0.23	0.08	0.65
40%Fe/MWCNT	0.03	0.73	0.22	0.98

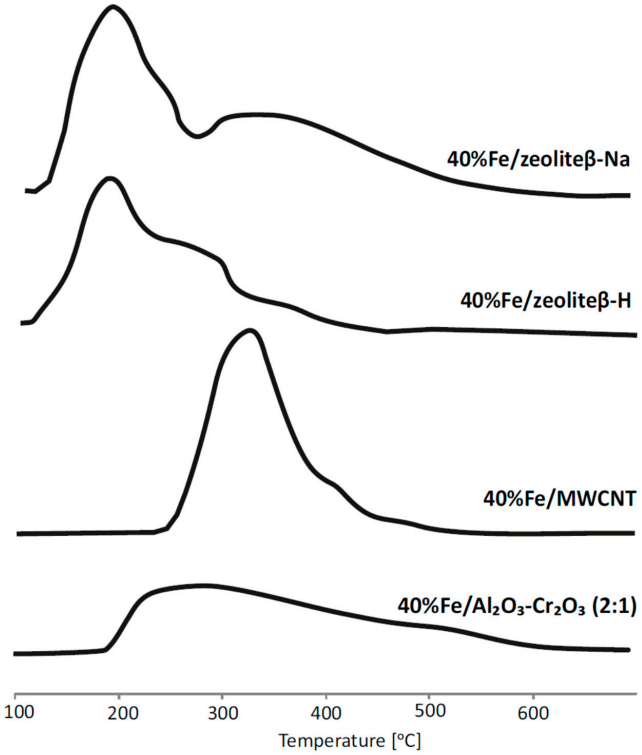

Figure 8. The temperature programmed desorption (TPD-NH_3) profiles collected for the reduced catalysts supported on binary oxide, MWCNTs, zeolite β-H -Na and zeolite β-H.

2.6. The Influence of the Carrier Type on the Catalyst Basicity

TPD-CO_2 measurements were done for all iron catalysts in the temperature range 100–900 °C and the results are presented in Table 5 and Figure 9, respectively. The obtained measurements performed

for the iron systems showed that the catalysts which exhibited the highest total acidity had the lowest basic properties. This tendency was observed for the rest of the investigated catalysts. One exception was the iron catalyst supported on multi-walled carbon nanotubes. This system exhibited the highest acidity as well as the highest basicity compared to other investigated catalysts. The obtained results may be related to the decomposition of the MWCNTs which took place during the temperature treatment of the studied catalyst [41,42].

Table 5. The amount of carbon dioxide adsorbed on the reduction at 500 °C in a mixture of 5%H_2-95%Ar and iron catalysts calculated from the surfaces under the TPD-CO_2 profiles.

Catalysts	Total Basicity (mmol·g^{-1})
40%Fe/$Al_2O_3Cr_2O_3$ (2:1)	1.16
40%Fe/Zeolite-H	1.10
40%Fe/Zeolite-Na	0.91
40%Fe/MWCNT	1.32

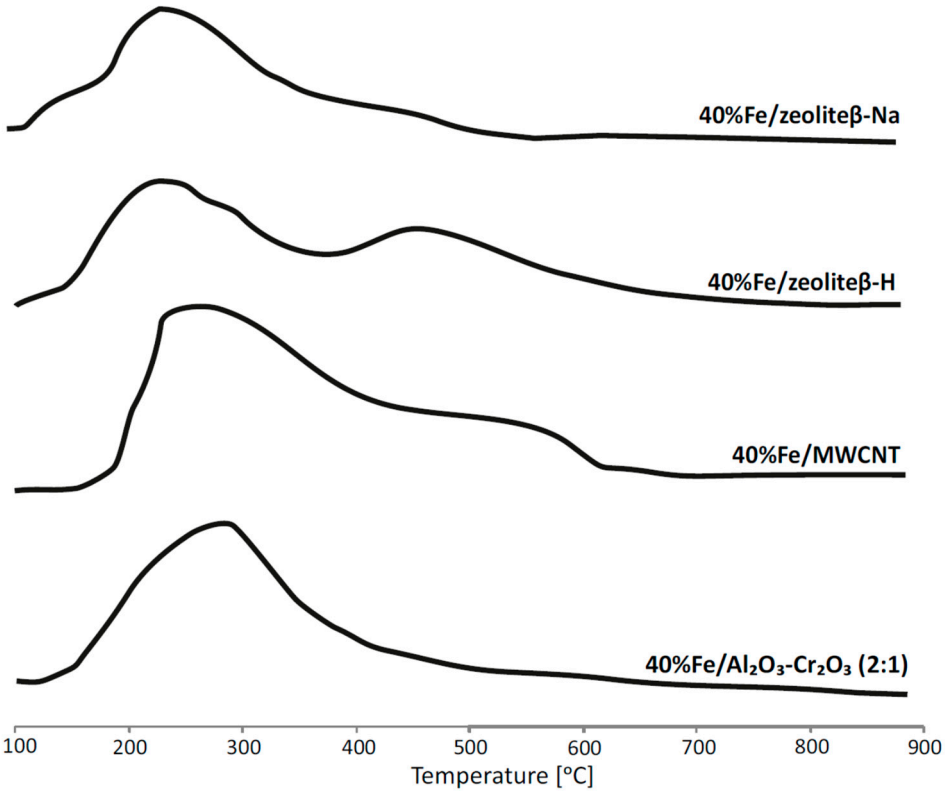

Figure 9. The TPD-CO_2 profiles recorded for reduction at 500 °C in a mixture of 5%H_2-95%Ar and iron catalysts supported on various carriers.

2.7. SEM-EDS Measurements of Iron Catalysts Supported on Two Types of Zeolites

The morphology of the prepared iron-based catalysts supported on Al_2O_3-Cr_2O_3 (2:1), zeolite β-H, and zeolite β-Na was investigated in order to elucidate the reasons for the differences in the activity of monometallic Fe catalysts in the F-T process. Both monometallic catalysts supported on the two types of zeolite were investigated. The investigated catalysts were calcined in an air atmosphere for 4 h and the results are presented in Figure 10. The performed SEM-EDS analysis of the surfaces of the catalyst confirmed the presence of Al, Si, O and Fe elements on their surface. The SEM-EDS analysis of the iron catalyst supported on zeolite β–Na confirmed the lack of sodium on the catalyst surface. This result can be explained by the detection limits of SEM-EDS technique. The only observed differences in the tested surfaces were the contents of the individual elements present on the catalyst

surface. In the case of the catalyst deposited on the sodium form of BEA zeolite, larger amounts of Fe were observed, which was confirmed by the XRD method. The 40%Fe/Al_2O_3-Cr_2O_3 (2:1) catalyst was also studied by this technique [2].

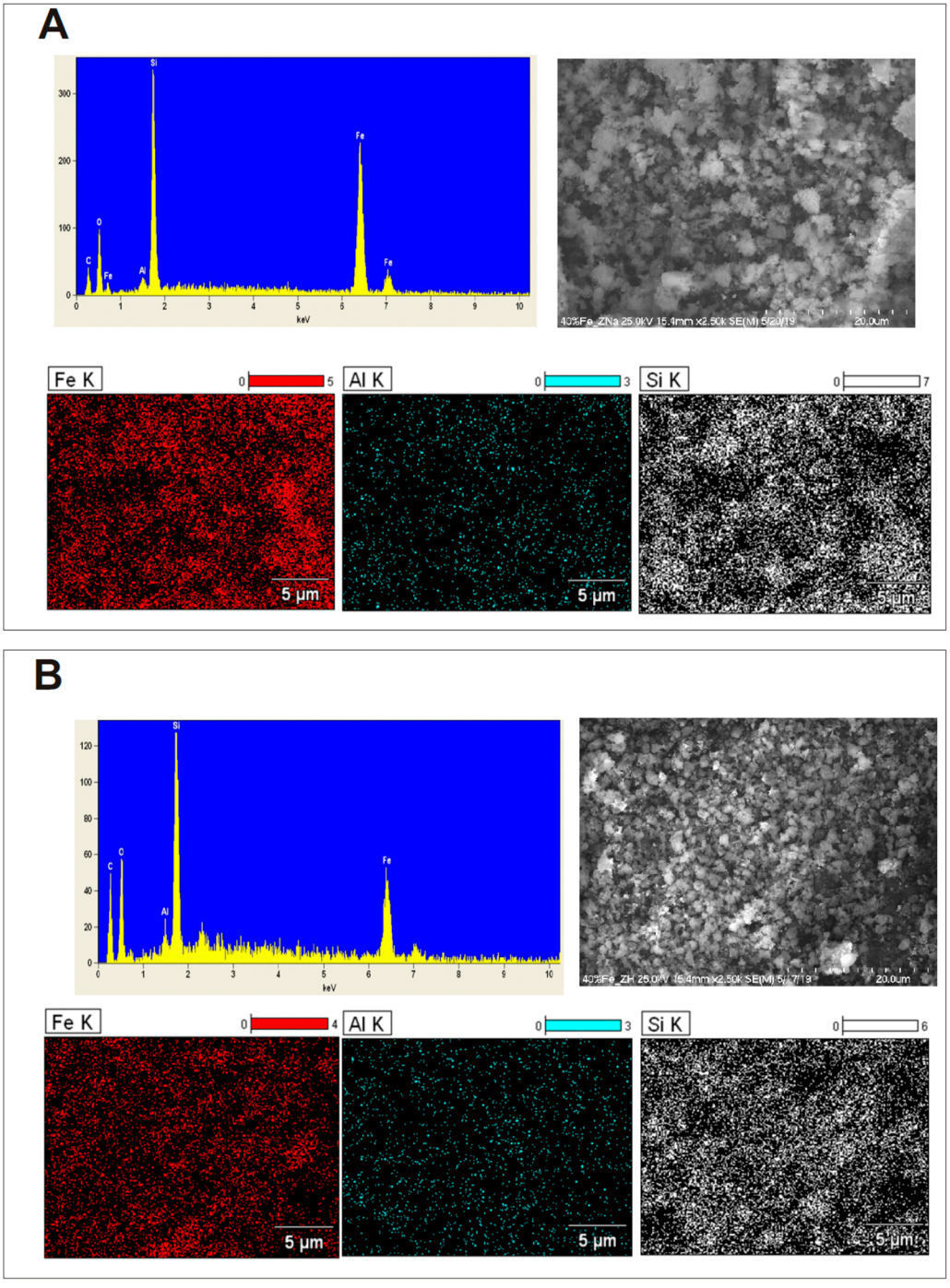

Figure 10. Scanning electron microscope images and EDX spectra collected for the investigated (**A**) 40%Fe/zeolite-β-Na and (**B**) 40%Fe/zeolite-β-H catalysts.

The SEM images collected for the 40%Fe/Al_2O_3-Cr_2O_3 (2:1) supported catalyst (results not shown in this paper) confirmed the composition of the prepared catalytic systems. Analysis of the elemental composition of the iron catalyst confirmed the highest quantity of the iron species present on the catalyst surface compared to the rest of the catalysts investigated in this work [2]. This phenomenon explained the activity row observed for the iron catalysts. It is also worth emphasizing that a similar tendency

was observed when comparing the discussed catalyst with other iron catalytic systems supported on binary oxide systems which are characterized by various molar ratios between Al and Cr [2].

3. Experimental

3.1. Supports and Catalysts Preparation

Binary oxide support was prepared according to our previous work [2]. In the case of the zeolite supports, the Zeolite β-Na form was purchased from HUTONG GLOBAL CO while the Zeolite β-H form was prepared using the ion exchange of the Zeolite β-Na which was transformed into a hydrogen form by the ion exchange method using ammonium nitrate (V). Zeolite β-Na was treated with a 1 M ammonium nitrate (V) solution at 80 °C for 2 h. Then the residue was filtered and washed with distilled water. Afterwards, the obtained material was dried at 105 °C for 4 h and then the obtained carrier material was calcined 4 h at 400 °C in an air atmosphere. MWCNTs were purchased from Sigma Aldrich (CAS:308068-56-6). Monometallic iron catalyst supported on MWCNTs, binary oxide Al_2O_3-Cr_2O_3 (2:1), Zeolite β-Na and Zeolite β-H were prepared by the conventional impregnation method using $Fe(NO_3)_3 \times 9H_2O$ as a precursor of the active phase. The monometallic Fe catalyst supported on Al_2O_3-Cr_2O_3 (2:1) was then dried in an air atmosphere at 120 °C and then calcined in the same atmosphere at 400 °C for 4 h. The Fe/MWCNT system was calcined in an argon stream for 4 h at 300 °C in order to avoid the oxidation process of the MWCNTs. Monometallic Fe catalysts supported on two kinds of zeolite were prepared analogously to the Fe/Al_2O_3-Cr_2O_3 (2:1) catalyst.

3.2. Characterization of the Catalytic Material

The specific surface area (SSA) and the pore size measurements of catalytic materials were investigated by the BET method based on the low temperature (77 K) nitrogen adsorption using ASAP 2020 Micrometrics (Surface Area and Porosity Analyzer, Micromeritics Instrument Corporation, Norcross, GA, USA). The pore size distributions were determined based on the BJH method. The distributions of the acids centres and total catalytic acidity of catalytic materials were studied using the TPD-NH_3 technique. Each catalytic system (about 0.2 g of the sample) was previously reduced in a mixture of 5%H_2-95%Ar at 500 °C for 1 h and then purified in the helium stream at 600 °C for 30 min^{-1}. Then the sample was cooled down to room temperature in a helium stream. In the next step, the physically adsorbed NH_3 was removed from the surface of the sample in the same atmosphere up to 100 °C. Then the chemisorbed NH_3 desorbed from the catalyst surface was monitored using a thermal-conductivity detector (TCD) during the heating of the sample from 100 to 600 °C. Temperature-programmed desorption of carbon dioxide measurements was performed in a quartz reactor using CO_2 as a probe molecule. The TPD-CO_2 experiments were done in the temperature range of 100–900. The TPD measurements were carried out after removing the CO_2 physisorbed on the catalyst surface. The reduction behaviour of the iron-containing system was investigated by TPR - H_2 technique. In all cases, the TPR-H_2 measurements were carried out using automatic AMI-1 equipment from the ambient to 900 °C. The heating rate in all measurements was 10 and 1 °C min^{-1} for the supports and Fe catalysts, respectively. The mass of the sample was about 0.1 g. During the TPR-H_2 measurements, the mixture of 5%H_2-95%Ar was used. To monitor the concentration of hydrogen, a thermal conductivity detector was applied. Phase composition studies of the calcined and reduced Fe catalysts were performed using a PANalyticalX'Pert Pro MPD diffractometer in the Bragg-Brentano reflecting geometry. Cu Kα radiation was used during all measurements. A PANalyticalX'Celerator detector was used in each experiment in the 2 Theta angles 5–90. Phase composition studies of the reduced catalytic system (5%H_2-95%Ar for 1 h at 500 °C) were performed using "ex situ" XRD measurements (Malvern Panalytical Ltd., Malvern, United Kingdom). In addition, XRD measurements were performed in the reaction chamber in the temperature range of 50–750 °C in a mixture of 5% H_2-95% Ar with a heating rate 10 °C per minute for a selected 40% Fe/MWCNT sample in order to understand its reduction mechanism. A Scanning Electron Microscope (SEM) (S-4700 HITACHI, Tokyo,

Japan) with an energy-dispersive detector (EDX) (ThermoNoran, Madison, WI, USA) was used in order to investigate the surface morphology of the Fe catalysts supported on various carrier materials. The X-ray spectra were used to determine the qualitative analysis of the surface of the catalytic materials. The distributions of each element on the catalytic surface were studied. The carbon deposition formed on the catalyst surface was determined by the TG-DTA-MS technique. Thermogravimetric analysis was carried out for catalysts after 20 h of operation in the reaction using a SETSYS 16/18 thermal analyzer from Setaram (Caluire, France) and a quadrupole mass spectrometer Balzers (Germany). The measurements were carried out in the temperature range of 20–1000 °C using a linear temperature rate of 10 °C/min. In all cases, the sample weight was about 10 mg in the dynamic conditions of a gas stream—Air (Air Products). The flow rate of the gas mixture was 40 cm^3/min in each experiment. The samples were outgassed before each measurement in order to be purified.

3.3. Catalytic Activity Measurements in the F-T Process

Hydrogenation of CO was performed using a high-pressure fixed bed reactor. A gas mixture of hydrogen and carbon monoxide with a molar ratio of 1 to 1 was used in the studies. The total flow of the reaction mixture in each catalytic test was 90 mL min^{-1}. The catalyst mass during the catalytic test was 2 g. The Fischer-Tropsch process was performed at 280 °C and at 30 atmospheres. Before the catalytic activity measurement, the catalyst was activated in a reaction mixture (50%H_2-50%CO for 1 h at 500 °C. The reactivity measurements were carried out after 20 h of the reaction. CO conversion and product distribution were determined using the GC-MS (Hewlett Packard 5890 SERIES II GCMS, United States of America) and GC techniques (equipped with a TCD or FID detector (Inco GC-505M Chromatograph, Poland)). All necessary information about the catalytic tests were also presented in our previous work [2,16]. In addition, in order to confirm our activity measurements analysis of the liquid hydrocarbons formed via the hydrogenation of CO, an IRTracer-100 FTIR (Shimadzu, Kyoto, Japan) spectrometer was used. The FTIR spectra's of the analysed products were obtained using an MCT detector. A resolution of 4.0 cm^{-1} and 128 scans were applied in each measurement. The "Specac" ATR accessory was used in each analysis.

4. Conclusions

F-T process performed on iron catalysts supported on various carriers prepared by the impregnation method was investigated. The results of the reactivity tests showed that the type of hydrocarbons formed in the hydrogenation of CO reaction depended strongly on the catalyst composition. The catalytic activity measurements indicated that the most active system in the studied process was the 40%Fe/Al_2O_3-Cr_2O_3 (2:1) catalyst. The hydrogenation of CO process performed at 30 atmospheres at a temperature of 280 °C confirmed that this system had high selectivity to linear hydrocarbons. In the case of this catalyst, the small quantity of unsaturated hydrocarbons formation was also detected. In addition, the 40%Fe/zeolite β-H catalyst was characterized by very high selectivity to linear hydrocarbons (94.8%) and to gasoline fraction. Iron catalyst supported on the Na-form of zeolite BEA was characterized by lowest selectivity to linear hydrocarbons (66.6%), but a higher yield for diesel fraction. The reaction performed on 40%Fe/MWCNT system mainly led to the diesel fraction production. The Fischer-Tropsch process conducted on the iron catalysts supported on MWCNTs and Al_2O_3-Cr_2O_3 (2:1) systems had the lowest amount of carbon deposit created on these catalytic material surfaces. These results confirm the possibility of using these systems for the CO hydrogenation process. It was also proven that the catalysts which showed the highest total acidity exhibited the highest CO conversion in the hydrogenation process and also high selectivity towards liquid product.

Supplementary Materials: The following are available online at http://www.mdpi.com/2073-4344/9/7/605/s1, Figure S1. Analysis of catalytic systems carried out in an air atmosphere in the temperature range 25-900°C for A) 40%Fe/Zeolite β-H and B) 40%Fe/Zeolite β-Na, Figure S2. Analysis of catalytic systems carried out in an air atmosphere in the temperature range 25-900°C for A) 40%Fe/MWCNT, B) 40%Fe/MWCNT (after reaction) and C) the mass spectrum of the gaseous decomposition products, Figure S3. Analysis of catalytic systems carried out in an air atmosphere in the temperature range 25-900°C for A) 40%Fe/ Al_2O_3-Cr_2O_3 (after reaction).

Author Contributions: Data curation, P.M.; Investigation, B.D., W.M., K.C.; P.M., W.M. performed XRD measurements, P.M. performed specific surface area measurements, K.C. performed TG-DTA-MS measurements, B.D. performed activity tests, TPR and TPD experiments; Methodology, Research consultation, M.I.S., K.V., I.W., Analysis of the SEM-EDS measurements, M.I.S.; Supervision, P.M., K.V. and M.I.S.; Visualization, P.M. and B.D.; Writing—Original draft, P.M.; Writing—Review & editing, P.M.

Funding: This work was partially funded from NCBiR-Grant no. BIOSTRATEG2/297310/13/NCBiR/2016.

Conflicts of Interest: The authors declare no conflict of interest.

References

1. Tijmensen, M.J.A.; Faaij, A.P.C.; Hamelinck, C.N.; van Hardeveld, M.R.M. Exploration of the possibilities for production of Fischer Tropsch liquids and power via biomass gasification. *Biomass Bioenergy* **2002**, *23*, 129–152. [CrossRef]
2. Mierczynski, P.; Dawid, B.; Maniukiewicz, W.; Mosinska, M.; Zakrzewski, M.; Ciesielski, R.; Kedziora, A.; Dubkov, S.; Gromov, D.; Rogowski, J.; et al. Fischer–Tropsch synthesis over various Fe/Al_2O_3–Cr_2O_3 catalysts. *React. Kinet. Mech. Catal.* **2018**, *124*, 545–561. [CrossRef]
3. Bukur, D.B.; Nowicki, L.; Manne, R.K.; Lang, X.S. Activation Studies with a Precipitated Iron Catalyst for Fischer-Tropsch Synthesis: II. Reaction Studies. *J. Catal.* **1995**, *155*, 366–375. [CrossRef]
4. Chalupka, K.A.; Maniukiewicz, W.; Mierczynski, P.; Maniecki, T.; Rynkowski, J.; Dzwigaj, S. The catalytic activity of Fe-containing SiBEA zeolites in Fischer–Tropsch synthesis. *Catal. Today* **2015**, *257*, 117–121. [CrossRef]
5. Peña, D.; Cognigni, A.; Neumayer, T.; van Beek, W.; Jones, D.S.; Quijada, M.; Rønning, M. Identification of carbon species on iron-based catalysts during Fischer-Tropsch synthesis. *Appl. Catal. A Gen.* **2018**, *554*, 10–23. [CrossRef]
6. Zhang, J.; Chen, J.; Ren, J.; Li, Y.; Sun, Y. Support effect of Co/Al_2O_3 catalysts for Fischer–Tropsch synthesis. *Fuel* **2003**, *82*, 581–586. [CrossRef]
7. Bezemer, G.L.; Bitter, J.H.; Kuipers, H.P.C.E.; Oosterbeek, H.; Holewijn, J.E.; Xu, X.; Kapteijn, F.; van Dillen, A.J.; de Jong, K.P. Cobalt Particle Size Effects in the Fischer−Tropsch Reaction Studied with Carbon Nanofiber Supported Catalysts. *J. Am. Chem. Soc.* **2006**, *128*, 3956–3964. [CrossRef]
8. Guczi, L.; Stefler, G.; Geszti, O.; Koppány, Z.; Kónya, Z.; Molnár, É.; Urbán, M.; Kiricsi, I. CO hydrogenation over cobalt and iron catalysts supported over multiwall carbon nanotubes: Effect of preparation. *J. Catal.* **2006**, *244*, 24–32. [CrossRef]
9. Bahome, M.C.; Jewell, L.L.; Hildebrandt, D.; Glasser, D.; Coville, N.J. Fischer–Tropsch synthesis over iron catalysts supported on carbon nanotubes. *Appl. Catal. A Gen.* **2005**, *287*, 60–67. [CrossRef]
10. Serp, P.; Corrias, M.; Kalck, P. Carbon nanotubes and nanofibers in catalysis. *Appl. Catal. A Gen.* **2003**, *253*, 337–358. [CrossRef]
11. Rodríguez-reinoso, F. The role of carbon materials in heterogeneous catalysis. *Carbon* **1998**, *36*, 159–175. [CrossRef]
12. Zhang, Z.; Zhang, J.; Wang, X.; Si, R.; Xu, J.; Han, Y.F. Promotional effects of multiwalled carbon nanotubes on iron catalysts for Fischer-Tropsch to olefins. *J. Catal.* **2018**, *365*, 71–85. [CrossRef]
13. Van Steen, E.; Prinsloo, F.F. Comparison of preparation methods for carbon nanotubes supported iron Fischer–Tropsch catalysts. *Catal. Today* **2002**, *71*, 327–334. [CrossRef]
14. Tao, Y.; Hattori, Y.; Matumoto, A.; Kanoh, H.; Kaneko, K. Comparative Study on Pore Structures of Mesoporous ZSM-5 from Resorcinol-Formaldehyde Aerogel and Carbon Aerogel Templating. *J. Phys. Chem. B* **2005**, *109*, 194–199. [CrossRef]
15. Chang, C.D.; Lang, W.H.; Silvestri, A.J. Synthesis gas conversion to aromatic hydrocarbons. *J. Catal.* **1979**, *56*, 268–273. [CrossRef]
16. Mierczynski, P.; Dawid, B.; Chalupka, K.; Maniukiewicz, W.; Witonska, I.; Szynkowska, M.I. Role of the activation process on catalytic properties of iron supported catalyst in Fischer-Tropsch synthesis. *J. Energy Inst.* **2019**. [CrossRef]
17. Cho, H.S.; Ryoo, R. Synthesis of ordered mesoporous MFI zeolite using CMK carbon templates. *Microporous Mesoporous Mater.* **2012**, *151*, 107–112. [CrossRef]

18. Caesar, P.D.; Brennan, J.A.; Garwood, W.E.; Ciric, J. Advances in Fischer-Tropsch chemistry. *J. Catal.* **1979**, *56*, 274–278. [CrossRef]
19. Nguyen-Ngoc, H.; Moller, K.; Ralek, M. Liquid Phase Synthesis of Aromates and Isomers on Polyfunctional Zeolitic Catalyst Mixtures. In *Studies in Surface Science and Catalysis*; Jacobs, P.A., Jaeger, N.I., Jírů, P., Kazansky, V.B., Schulz-Ekloff, G., Eds.; Elsevier: Amsterdam, The Netherlands, 1984; Volume 18, pp. 291–297.
20. Chum, H.L.; Overend, R.P. Biomass and renewable fuels. *Fuel Process. Technol.* **2001**, *71*, 187–195. [CrossRef]
21. Moodley, D.J.; van de Loosdrecht, J.; Saib, A.M.; Overett, M.J.; Datye, A.K.; Niemantsverdriet, J.W. Carbon deposition as a deactivation mechanism of cobalt-based Fischer–Tropsch synthesis catalysts under realistic conditions. *Appl. Catal. A Gen.* **2009**, *354*, 102–110. [CrossRef]
22. Maniecki, T.; Stadnichenko, A.; Maniukiewicz, W.; Bawolak, K.; Mierczynski, P.; Boronin, A.; Jozwiak, W. An active phase transformation on surface of Ni-Au/Al_2O_3 catalyst during partial oxidation of methane to synthesis gas. *Kinet. Catal.* **2010**, *51*, 573–578. [CrossRef]
23. Niemantsverdriet, J.W.; Van der Kraan, A.M.; Van Dijk, W.L.; Van der Baan, H.S. Behavior of metallic iron catalysts during Fischer-Tropsch synthesis studied with Moessbauer spectroscopy, x-ray diffraction, carbon content determination, and reaction kinetic measurements. *J. Phys. Chem.* **1980**, *84*, 3363–3370. [CrossRef]
24. Menon, P.G. Coke on catalysts-harmful, harmless, invisible and beneficial types. *J. Mol. Catal.* **1990**, *59*, 207–220. [CrossRef]
25. Sai Prasad, P.S.; Bae, J.W.; Jun, K.-W.; Lee, K.W. Fischer–Tropsch Synthesis by Carbon Dioxide Hydrogenation on Fe-Based Catalysts. *Catal. Surv. Asia* **2008**, *12*, 170–183. [CrossRef]
26. De Bokx, P.K.; Kock, A.J.H.M.; Boellaard, E.; Klop, W.; Geus, J.W. The formation of filamentous carbon on iron and nickel catalysts: I. Thermodynamics. *J. Catal.* **1985**, *96*, 454–467. [CrossRef]
27. Zhang, C.; Zhao, G.; Liu, K.; Yang, Y.; Xiang, H.; Li, Y. Adsorption and reaction of CO and hydrogen on iron-based Fischer–Tropsch synthesis catalysts. *J. Mol. Catal. A Chem.* **2010**, *328*, 35–43. [CrossRef]
28. Maniecki, T.; Mierczynski, P.; Maniukiewicz, W.; Bawolak, K.; Gebauer, D.; Jozwiak, W. Bimetallic Au-Cu, Ag-Cu/$CrAl_3O_6$ Catalysts for Methanol Synthesis. *Catal. Lett.* **2009**, *130*, 481–488. [CrossRef]
29. Maniecki, T.P.; Bawolak, K.; Gebauer, D.; Mierczynski, P.; Jozwiak, W.K. Catalytic activity and physicochemical properties of Ni-Au/Al_3CrO_6 system for partial oxidation of methane to synthesis gas. *Kinet. Catal.* **2009**, *50*, 138–144. [CrossRef]
30. Maniecki, T.; Mierczynski, P.; Bawolak, K.; Lesniewska, E.; Rogowski, J.; Jozwiak, W. Characterization of Cu-(Ag, Au)/$CrAl_3O_6$ Methanol Synthesis Catalysts by TOF-SIMS and SEM-EDS Techniques. *Pol. J. Chem.* **2009**, *83*, 1643–1651.
31. Mierczynski, P.; Maniecki, T.; Maniukiewicz, W.; Jozwiak, W. Cu/Cr_2O_3 center dot $3Al_2O_3$ and Au-Cu/Cr_2O_3 center dot $3Al_2O_3$ catalysts for methanol synthesis and water gas shift reactions. *React. Kinet. Mech. Catal.* **2011**, *104*, 139–148. [CrossRef]
32. Maniecki, T.P.; Bawolak, K.; Mierczyński, P.; Jozwiak, W.K. Development of Stable and Highly Active Bimetallic Ni–Au Catalysts Supported on Binary Oxides $CrAl_3O_6$ for POM Reaction. *Catal. Lett.* **2008**, *128*, 401. [CrossRef]
33. Jozwiak, W.K.; Kaczmarek, E.; Maniecki, T.P.; Ignaczak, W.; Maniukiewicz, W. Reduction behavior of iron oxides in hydrogen and carbon monoxide atmospheres. *Appl. Catal. A Gen.* **2007**, *326*, 17–27. [CrossRef]
34. Maniecki, T.; Mierczynski, P.; Maniukiewicz, W.; Gebauer, D.; Jozwiak, W. The effect of spinel type support $FeAlO_3$, $ZnAl_2O_4$, $CrAl_3O_6$ on physicochemical properties of Cu, Ag, Au, Ru supported catalysts for methanol synthesis. *Kinet. Catal.* **2009**, *50*, 228–234. [CrossRef]
35. Jozwiak, W.; Maniecki, T.; Mierczynski, P.; Bawolak, K.; Maniukiewicz, W. Reduction Study of Iron-Alumina Binary Oxide $Fe_{2-x}Al_xO_3$. *Pol. J. Chem.* **2009**, *83*, 2153–2162.
36. Mierczynski, P.; Vasilev, K.; Mierczynska, A.; Maniukiewicz, W.; Szynkowska, M.I.; Maniecki, T.P. Bimetallic Au-Cu, Au-Ni catalysts supported on MWCNTs for oxy-steam reforming of methanol. *Appl. Catal. B Environ.* **2016**, *185*, 281–294. [CrossRef]
37. Mierczynski, P.; Vasilev, K.; Mierczynska, A.; Maniukiewicz, W.; Ciesielski, R.; Rogowski, J.; Szynkowska, I.M.; Trifonov, A.Y.; Dubkov, S.V.; Gromov, D.G.; et al. The effect of gold on modern bimetallic Au-Cu/MWCNT catalysts for the oxy-steam reforming of methanol. *Catal. Sci. Technol.* **2016**. [CrossRef]
38. Lu, Y.; Yan, Q.; Han, J.; Cao, B.; Street, J.; Yu, F. Fischer–Tropsch synthesis of olefin-rich liquid hydrocarbons from biomass-derived syngas over carbon-encapsulated iron carbide/iron nanoparticles catalyst. *Fuel* **2017**, *193*, 369–384. [CrossRef]

39. Wezendonk, T.A.; Sun, X.; Dugulan, A.I.; van Hoof, A.J.F.; Hensen, E.J.M.; Kapteijn, F.; Gascon, J. Controlled formation of iron carbides and their performance in Fischer-Tropsch synthesis. *J. Catal.* **2018**, *362*, 106–117. [CrossRef]
40. Chalupka, K.A.; Casale, S.; Zurawicz, E.; Rynkowski, J.; Dzwigaj, S. The remarkable effect of the preparation procedure on the catalytic activity of CoBEA zeolites in the Fischer–Tropsch synthesis. *Microporous Mesoporous Mater.* **2015**, *211*, 9–18. [CrossRef]
41. Mierczynski, P.; Ciesielski, R.; Kedziora, A.; Nowosielska, M.; Kubicki, J.; Maniukiewicz, W.; Czylkowska, A.; Maniecki, T. Monometallic copper catalysts supported on multi-walled carbon nanotubes for the oxy-steam reforming of methanol. *React. Kinet. Mech. Catal.* **2015**, 1–17. [CrossRef]
42. Mierczynski, P.; Mierczynska, A.; Maniukiewicz, W.; Maniecki, T.P.; Vasilev, K. MWCNTs as a catalyst in oxy-steam reforming of methanol. *RSC Adv.* **2016**, *6*, 81408–81413. [CrossRef]